Ultrasonics Sonochemistry 112 (2025) 107171

Contents lists available at ScienceDirect

Ultrasonics Sonochemistry

journal homepage: www.elsevier.com/locate/ultson

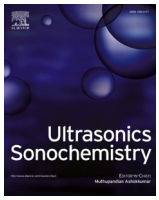

Dominant spoilage bacteria in crayfish alleviate ultrasonic stress through mechanosensitive channels but could not prevent the process of membrane destruction

Zechuan Dai [a,c,d], Lingyun Meng [a,c,d], Sai Wang [a,c,d], Jiao Li [a,c,d,*], Xiangzhao Mao [a,b,c,d,*]

[a] State Key Laboratory of Marine Food Processing and Safety Control, College of Food Science and Engineering, Ocean University of China, Qingdao 266404, PR China
[b] Laboratory for Marine Drugs and Bioproducts of Qingdao National Laboratory for Marine Science and Technology, Qingdao 266237, PR China
[c] Qingdao Key Laboratory of Food Biotechnology, Qingdao 266404, PR China
[d] Key Laboratory of Biological Processing of Aquatic Products, China National Light Industry, Qingdao 266404, PR China

ARTICLE INFO

Keywords:
Ultrasonic stress
Shewanella baltica
Aeromonas veronii
Stress response
Membrane destruction
Mechanosensitive channels

ABSTRACT

Although there have been many studies on the efficacy of ultrasonic inactivation, the stress resistance mechanism of bacteria is still a challenge for complete ultrasonic inactivation. In this study, the dominant spoilage bacteria in crayfish, *Shewanella baltica* (*S. baltica*) and *Aeromonas veronii* (*A. veronii*), were subjected to high-intensity ultrasonic treatment. The results showed compromised cell membrane, decreased membrane fluidity, hyperpolarized membrane potential, and disrupted succinate-coenzyme Q reductase. Transmission electron microscopy revealed significant fragmentation of *S. baltica*, whereas *A. veronii*, with its thick cell wall and outer capsule membrane, demonstrated enhanced resistance to ultrasound. Real-time quantitative PCR indicated that in response to ultrasonic stress, bacteria initiated a stress response mechanism by increasing the expression of mechanosensitive channels; meanwhile, the outer capsule of *A. veronii* delayed the transformation of ultrasonic external forces into cell membrane stress. The study found that in response to ultrasonic stress, bacteria initiated a stress response mechanism by increasing the expression of mechanosensitive channels as "emergency valve" in short time but could not prevent the process of membrane destruction with prolonged exposure. This finding provided a basis for addressing bacterial stress tolerance in ultrasonic inactivation.

1. Introduction

In 2020, global aquaculture production reached more than 122 million tonnes, valued at USD 299.9 billion [1]. As a rich source of high-quality proteins, aquatic products have become an indispensable and popular food worldwide. However, aquatic products are easily infected by microorganisms during storage and distribution, resulting in spoilage and increased food safety risks. This bottleneck restricts the development of the aquatic industry [2]. Throughout the decay process of aquatic products, one or a few types of bacteria, known as dominant spoilage bacteria, usually dominate significantly in quantity and play a vital role in the decay process [3]. *Shewanella baltica* (*S. baltica*) and *Aeromonas veronii* (*A. veronii*) are typical dominant spoilage bacteria, which can cause the spoilage of *Aristichthys nobilis*, *Ctenopharyngodon idellus*, *Lateolabrax Japonicus* and other high-value aquatic products [4–6]. In our previous studies, *S. baltica* and *A. veronii* were confirmed as the dominant spoilage organisms, with the largest relative abundance at the end of crayfish spoilage [7]. To preserve the quality of aquatic products throughout storage, it is crucial to effectively reduce or eliminate dominant spoilage bacteria.

As an alternative to conventional preservation methods, nonthermal processing techniques such as ultrasound, ultra-high pressure, irradiation, magnetic field, and cold plasma treatments can limit the growth of spoilage organisms without compromising the sensory properties or nutritional components of aquatic products [8,9]. Currently, the bactericidal efficacy of ultrasound is widely accepted as the cavitation effect [10,11], which indicated that the intense shear force produced by shockwaves or microjets impacts cells externally and internally, leading

* Corresponding authors at: State Key Laboratory of Marine Food Processing and Safety Control, College of Food Science and Engineering, Ocean University of China, Qingdao 266404, PR China.
E-mail addresses: lijiao@ouc.edu.cn (J. Li), xzhmao@ouc.edu.cn (X. Mao).

https://doi.org/10.1016/j.ultsonch.2024.107171
Received 10 October 2024; Received in revised form 14 November 2024; Accepted 21 November 2024
Available online 24 November 2024

to thinner cell walls and perforated cell membranes [12–14]. Despite many studies on the efficacy of ultrasonic treatment for bacterial inactivation, the stress resistance mechanisms of bacteria have remained an obstacle to realize complete inactivation [15,16]. So it is crucial to study the response mechanisms of bacteria to ultrasonic stress. According to the cell membrane stress transformation theory, cell membrane could absorb mechanical energy from the ultrasound field and transform it into stress of the intramembrane [17]. Mechanosensitive ion channels facilitate the transmission of mechanical signals within and outside cells by detecting changes in cell membrane tension [18]. Therefore, it is necessary to further explore whether the bacteria will regulate the expression of mechanosensitive ion channels to enhance their adaptability under ultrasound stress. The investigation of bacterial resistance mechanisms to ultrasonic stress will help to optimize the ultrasonic inactivation process and improve inactivation efficiency.

In this study, the dominant spoilage bacteria, *S. baltica* and *A. veronii*, previously identified in crayfish, were subjected to ultrasonic treatment. *S. baltica* is a gram-negative, psychrophilic bacterium that reduces trimethylamine oxide to trimethylamine and produces H_2S, causing sour and off-odors in aquatic products. *A. veronii* is a gram-negative, facultative anaerobic bacterium with a narrow capsule and strong environmental adaptability, capable of causing human gastroenteritis, peritonitis, sepsis, and trauma infections. The study by Gao et al. [19] suggested that the primary cause of bacterial resistance to ultrasonic deactivation lies in the characteristics of the outer capsule. We assume that the differences in cell envelope of *S. baltica* and *A. veronii* may result in varying effects on ultrasonic inactivation.

In order to explore the varying effects of different cell envelope on ultrasonic inactivation, we examined the changes in cell membrane fluidity, membrane potential, and membrane-bound enzyme activity of *S. baltica* and *A. veronii*. In addition, transmission electron microscopy (TEM) was employed to examine the microstructural changes in bacteria after ultrasonic treatment. Real-time quantitative PCR was employed to investigate the expression levels of mechanosensitive channels induced by ultrasound and to elucidate the underlying stress response mechanisms.

2. Materials and methods

2.1. Preparation of bacterial suspension

Shewanella baltica (*S. baltica*) and *Aeromonas veronii* (*A. veronii*) were the dominant spoilage bacteria in crayfish previously screened in our laboratory. The strain was preserved in a glycerol tube at −80 °C and inoculated into a nutrient broth medium for bacterial culture. It was streaked and purified on trisaccharide iron agar medium and *Aeromonas* basic medium to obtain single colonies. The bacterial suspension was adjusted to 10^8 CFU/mL.

2.2. Ultrasonic treatment

Ultrasonic treatment was conducted using an ultrasonicator (Scientz-IID, Ningbo Scientz Biotechnology Co., China). Bacterial suspensions of 40 mL were placed in 50 mL columniform centrifuge tubes and subjected to ultrasonic irradiation emitted through a 10-mm-diameter tip with a power of 400 W. The ultrasonic probe tip was positioned 2 cm below the surface of the bacterial suspensions, pulse interval of 2 s on, 2 s off. The sample was placed in an ice bath to maintain the solution temperature below 25 °C during the experiment.

2.3. Evaluation of the inactivation effect of ultrasound on spoilage bacteria

The plate counting method was employed to assess the viability of *S. baltica* and *A. veronii* following ultrasound exposure. Bacterial suspensions were 10-fold diluted with sterile saline solution, and 100 μL of the diluted *S. baltica* suspension was plated onto triple sugar iron agar and 100 μL of *A. veronii* bacterial suspension was plated onto *Aeromonas* medium base agar, then the plate was placed in the incubator at 30℃ for 24 h. Each result was the geometrical mean of at least three counts.

2.4. Analysis of alterations in the structural components of the cell membrane

The completely dried samples were mixed with a specific quantity of dried potassium bromide before being thoroughly ground under an infrared baking lamp. After grinding, the mixed powder was compressed into a uniform circular thin sheet using a tablet press and then measured using a fourier transform infrared spectrophotometer (Nicolet iS10, Thermo Fisher Scientific, USA). The instrument parameters were set: the scanning range was 400 cm^{-1} to 4000 cm^{-1}.

2.5. Determination of integrity of cell membrane

The integrity of the cell membrane was assessed according to the method described by Kim and Kang [20] with some adjustments. The analysis was conducted using flow cytometry (BD FACSVerse, Becton, Dickinson and Company, USA), with the following parameters: an excitation wavelength of 535 nm, an emission wavelength of 620 nm, collection of 10,000 cells at a low flow rate, and the generation of scatter plots and histograms.

2.6. Detection of cells membrane fluidity

Membrane fluidity was detected with 8-Anilino-1-naphthalenesulfonic acid (ANS) fluorescence [21]. The ANS fluorescence intensity of each incubate was determined by the fluorescence spectrophotometer (SpectraMax iD3; Molecular Device, Sunnyvale, USA). The excitation wavelength is set at 385 nm, the emission wavelength is 480 nm, and the emission spectrum range is 400 nm to 650 nm.

2.7. Assessment of succinate-coenzyme Q reductase (SQR) activity

SQR activity was analyzed to evaluate cell proliferation following ultrasound treatment, using the method described by Kim and Kang [20,22]. Briefly, 100 μL iodonitrotetrazolium chloride solution (0.5 %) was added to 0.9 mL of the treated sample, and the mixture was incubated at 37 °C for 2 h in the dark. Bacterial cells were washed three times, followed by resuspension in 1 mL 1:1(v/v) acetone-ethanol. The formazan produced was quantitatively assessed by measuring its absorbance at 490 nm.

2.8. Transmission electron microscopy (TEM) analyis

The samples before and after ultrasonic treatment were placed in a 2.0 mL centrifuge tube, centrifuged at 4 °C, 6000 r/min for 8 min, and the bacterial precipitate was collected. The precipitate was washed three times with 0.85 % normal saline and then fixed overnight in 2.5 % glutaraldehyde. Post-washing with phosphate buffer solution, the bacteria were additionally fixed with 0.1 M osmium tetroxide for 1.5 h. The fixed sample underwent dehydration in ethanol, was washed with acetone, and embedded in resin overnight at 65 °C. Following sectioning, the slices were sequentially stained with 2 % uranyl acetate and Reynold's lead citrate. Finally, the cells were examined using a 120-kV TEM (JEM-1200EX, JEOL, Japan).

2.9. Assay of the membrane potential

The cell membrane potential was measured according to the instruction of the BacLightTM Bacterial Membrane Potential Kit (Invitrogen, Grand Island, NY, United States). Briefly, cells were grown at 37 °C to an optical density of 0.5 at 600 nm, then harvested by

centrifugation (5000 × g, 5 min) and washed twice with PBS (pH 7.0). Next, 1 mL of cell suspensions were placed in black centrifuge tube for 30 min at 37 °C, then 10 μL of the membrane potential-sensitive fluorescent probe 3,30 −diethyloxacarbocyanine iodide [$DiOC_2(3)$] was added and incubated for 30 min at 37 °C, followed by addition of citral. The depolarized control treatment was added 10 μL of 500 μM carbonyl cyanide 3-chlorophenylhydrazone (CCCP). Fluorescence was measured at excitation and emission wavelengths 492 and 515 nm.

2.10. Quantitative real-time PCR

qPCR was employed to analyze the transcription of sensitive ion channel proteins and energy metabolism genes in bacteria following ultrasound exposure. Total RNA was extracted from bacteria under both normal conditions and in the presence of ultrasound. Primers, Primer Mix, SYBR Green Mix, and nuclease-free H_2O were added, and the mixture was evenly mixed and analyzed with a fluorescence quantitative PCR instrument. The program was set as a two-step real-time quantification method, and the pre-denaturation was 95℃ for 10 min. After that, 40 cycles of denaturation at 95℃ for 15 s and annealing extension at 63℃ for 30 s were carried out in each step. Fluorescence values were read at the extension stage each time. After the cycle, solubilization curves were prepared and the expression levels of selected target genes were calculated by $2^{-\Delta\Delta Ct}$ methods. The primer sequences of target genes are shown in Table 1and Table 2.

2.11. Statistical analysis

All experiments were conducted at least three times, and data were analyzed using SPSS 26.0 software (SPSS Inc., Chicago, IL, USA). Statistical significance was determined by ANOVA test followed by Tukey's post hoc test. $P < 0.05$ was considered statistically significant.

3. 3.Results and discussions

3.1. Inactivation effect of ultrasound on S. baltica and A. veronii

The inactivation effects of ultrasound on *S. baltica* and *A. veronii* are summarized in Table 3. The results revealed that the bactericidal effect of ultrasound on bacteria increased gradually with prolonged exposure time. After 15 min of ultrasonic treatment with a power of 400 W, the total colony count of *S. baltica* and *A. veronii* decreased by 5.77 log CFU/mL and 2.56 log CFU/mL. Cameron et al. [23] observed an inactivation effect on *Escherichia coli* of 3.88 log CFU/mL when the power was 750 W and the ultrasonic exposure time was 10 min, while Li et al. [12] reported an inactivation effect on *Staphylococcus aureus* of 1.14 log CFU/mL when the power was 300 W and the ultrasonic exposure time was 20 min. Comparison with previous studies revealed that ultrasound exhibited a favorable bactericidal effect on both *S. baltica* and *A. veronii*. In addition, we observed significant differences in the bactericidal effects of ultrasound on the two bacterial strains. *S. baltica* exhibited greater sensitivity to ultrasound pressure, while *A. veronii* with its coccoid or short rod-shaped morphology, demonstrated greater resilience to adverse ultrasound conditions compared to the elongated rod-shaped *S. baltica*. Spherical bacteria had a more uniform distribution of mechanical forces and a smaller surface area-to-volume ratio, which could reduce the impact of ultrasonic waves [24]. Liao et al. [25] also reported that cell shape played a significant role in ultrasonic resistance, with the spherical shape of *S. aureus* potentially aiding in their defense against ultrasonic stress.

Table 1
Amplification primers of *S. baltica* target genes.

Gene name	Amplification primers (From 5′to 3′)
mscS	CCCAAGGGCGCACGATAAAGTC
	CCCAAGGGCGCACGATAAAGTC
mscL	GACGCGCCTTCTGTGGTGATTG
	GGTGCTTTAGGCGCGACTTCTTCT
sucC	GGTGCTTTAGGCGCGACTTCTTCT
	GGTGCTTTAGGCGCGACTTCTTCT
sdhA	CGCAGCGGGTCAGCATTTAGGT
	CAACGATTCAGACGCGCCAGAGAT

Table 2
Amplification primers of *A. veronii* target genes.

Gene name	Amplification primers (From 5′to 3′)
mscK	AGTGGGTAGCGGGTGGTCTGT
	AGCTGCTGGTTGGGGATGA
mscM	TCAAGACCCGGGCAACCACCATAG
	GGCGTCGGCGTCTCCAATACCAG
mscL	AGTGGGTAGCGGGTGGTCTGT
	AGCTGCTGGTTGGGGATGA
sucC	AGTGGCCAAGAGCAAGGATGAGAT
	CCACGGCGCCCAGGTAGAG
sdhA	TGGGGCCCGCACATCAAG
	CTCGCCCACCGCAAACAGAC

Table 3
Inactivation effect of ultrasound on *S. baltica and A. veronii.*

Time (min)	Log reduction (Log_{10} CFU/mL)	
	Shewanella baltica	*Aeromonas veronii*
2.5	$2.41 \pm 0.13^{f,A}$	$0.49 \pm 0.09^{f,B}$
5	$3.61 \pm 0.25^{e,A}$	$0.98 \pm 0.14^{e,B}$
7.5	$4.21 \pm 0.38^{d,A}$	$1.68 \pm 0.23^{d,B}$
10	$4.96 \pm 0.23^{c,A}$	$1.96 \pm 0.33^{c,B}$
12.5	$5.51 \pm 0.28^{b,A}$	$2.32 \pm 0.22^{b,B}$
15	$5.77 \pm 0.41^{a,A}$	$2.56 \pm 0.19^{a,B}$

* Significant differences at the $P < 0.05$ level are indicated by different lowercase letters in each column and by different uppercase letters in each row.

3.2. Changes of cell membrane integrity of S. baltica and A. veronii

The integrity of the bacterial membrane is vital for bacterial survival. In this study, propidium iodide (PI) was used to examine cell membrane damage resulting from ultrasound treatment. was utilized to investigate the impact of ultrasound on the integrity of the bacterial cell membrane. While PI cannot penetrate intact cell membranes, it could permeate damaged cell membranes and stain the nucleus [26]. Therefore, the integrity of the cell membrane can be inferred from the percentage of red fluorescent cells [27]. As illustrated in Fig. 1 (A, B), ultrasonic treatment had the potential to disrupt the integrity of bacterial cell membranes. The proportion of PI-stained cells in *S. baltica* increased from 1.23 % in the control group to 33.37 %, and in *A. veronii*, it increased from 3.75 % in the control group to 53.52 %. This significant rise confirmed the pronounced disruptive effect of ultrasound on cell membrane integrity, enabling PI penetration into the bacteria's interior and subsequent staining. Interestingly, we observed that the proportion of PI-stained cells peaked after 2.5 min of ultrasound treatment and gradually decreased with prolonged ultrasound exposure. This trend indicated that brief ultrasound exposure durations might induce cell membrane disruption, whereas prolonged exposures could lead to cell death, releasing a significant amount of intracellular nucleic acid, which ultimately prevented PI dye from binding [11].

3.3. Changes of cell membrane composition induced by ultrasound treatment

FTIR analysis was used to determine changes in cell membrane composition after ultrasonic treatment by comparing spectra of treated and control samples (Fig. 2). As the duration of ultrasonic treatment increased, at the peak intensity 1080 cm^{-1} and 1240 cm^{-1} increased,

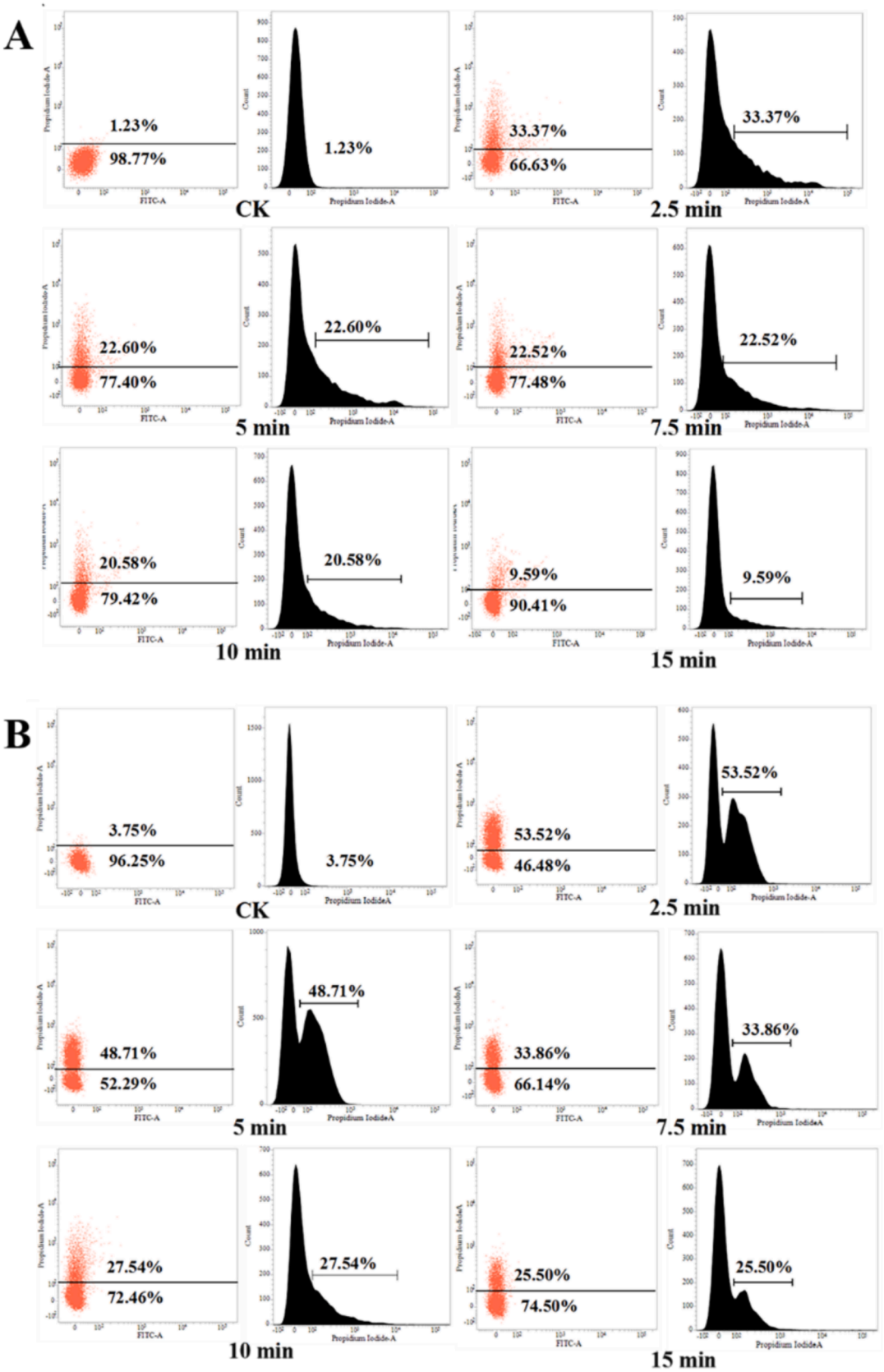

Fig. 1. PI staining of *S. baltica* (A) and *A. veronii* (B) after ultrasonic treatment.

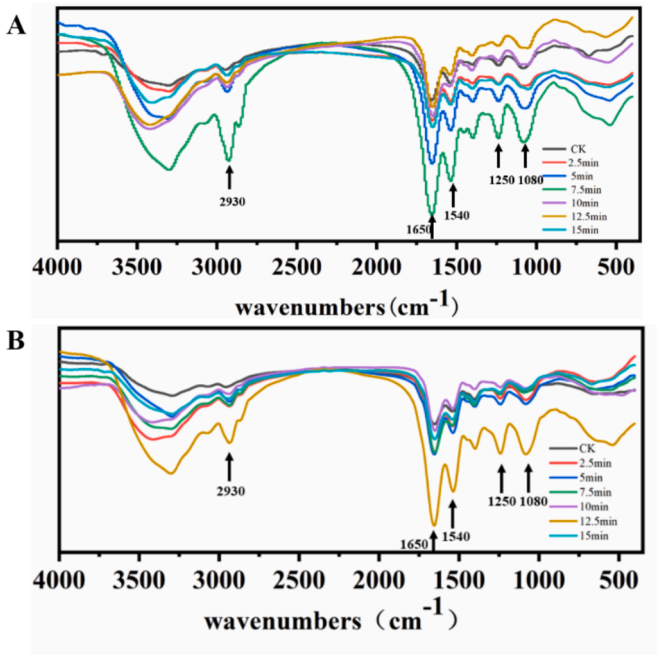

Fig. 2. FTIR figures of *S. baltica* (A) and *A. veronii* (B).

attributed to the influence of ultrasound on phospholipids content within the bacterial cell membrane [28,29]. The samples after ultrasonication displayed a significantly enhanced absorption peak at the amido-1 bond (1540 cm^{-1}, 1650 cm^{-1}), possibly resulting from alterations in protein conformation on the cell membrane and the exposure of amide groups. Furthermore, an elevation in peak intensity at 2930 cm^{-1} was noted in the bacteria post-treatment, which could be ascribed to an augmented fatty acid content. The speculated increase in fatty acid content was attributed to the disruption of the phospholipid bilayer arrangement within the cell membrane induced by ultrasound [30]. This disruption exposed the hydrophobic groups of fatty acids, providing further evidence of bacterial membrane disruption. Based on the aforementioned findings, the results of FTIR analysis further substantiated that ultrasound induced bacterial death by disrupting cell membrane structure and altering cell membrane composition.

3.4. Effect of ultrasonic treatment on energy metabolism on cell membrane

Numerous enzymes on the bacterial cell membrane played pivotal roles in bacterial life activities. SQR was an enzyme involved in energy metabolism within the electron transport chain. Its activity served as a reflection of the integrity of the energy metabolism process. The impact of ultrasonic treatment on SQR activity was depicted in Fig. 3, revealing a significant reduction in SQR activity in both bacteria with increasing ultrasonic treatment time. This suggested that the free radicals produced by ultrasound could compromise the life activities of bacteria by inhibiting the internal energy metabolism process, ultimately leading to bacterial death. The reason why ultrasound had such a significant inhibitory effect on SQR enzyme activity may have been due to the massive production of ROS during ultrasound treatment. ROS formation specifically induced a mutation in SQR, resulting in impaired electron transfer to ubiquinone, thus hindering energy production via both the TCA cycle [31]. Li et al. [32] proposed a mechanism whereby free radicals generated by ultrasonic cavitation potentially enter cells through activated mechanosensitive channels, resulting in an increase in intracellular ROS levels. Jeon and Ha [33] reported that the loss of SQR activity was primarily due to ROS stress. This similar conclusion was summarized by Kim and Dong [20] when they studied the effect of blue

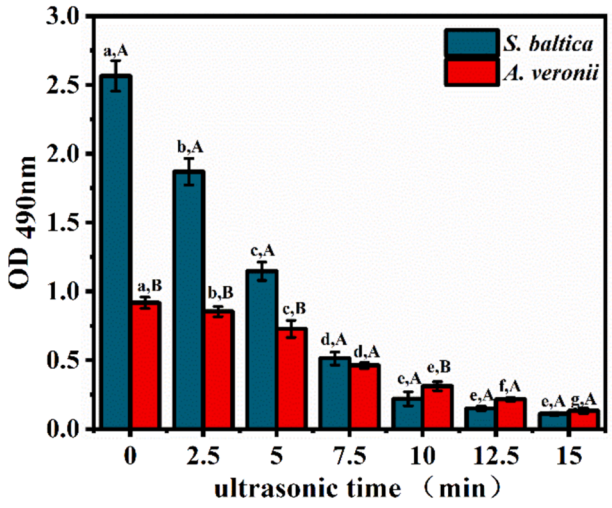

Fig. 3. Effect of ultrasound on the SQR activity of *S. baltica* and *A. veronii.*

light on SQR enzyme activity of *Escherichia coli O157:H7*. Nevertheless, as the duration of ultrasonic treatment increased, ROS levels steadily declined, likely due to the progressive breakdown of intracellular ROS in solution post-bacterial lysis, which could be attributed to their inherent instability.

3.5. Changes of the cell membrane potential by ultrasound treatment

The cell membrane potential is essential for normal energy transduction, serving as a key indicator of cellular physiological activity [34]. The fluorescent $DiOC_2(3)$ exhibited green fluorescence in all cells. However, as the membrane potential increased, a large proton gradient formed within the cells. Under these conditions, $DiOC_2(3)$ underwent self-binding and gradual accumulation, causing the fluorescence color to shift gradually from green to red. Fig. 4 illustrated the changes in membrane potential of the bacteria after sonication, with the membrane potential of depolarized bacteria after CCCP treatment serving as a control. It was evident that the ratio of red to green fluorescence gradually increased with the extension of sonication time. These findings suggested that ultrasound increased the membrane potential of bacteria, resulting in hyperpolarization and impacting the normal physiological metabolic activities of bacteria. The phenomenon of bacterial

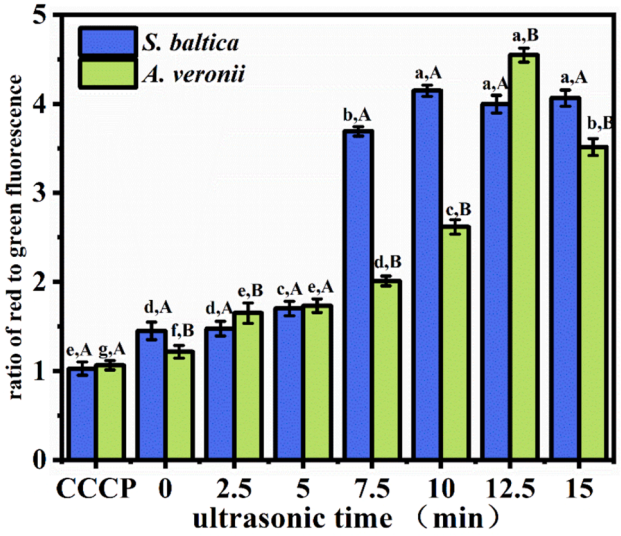

Fig. 4. Effect of ultrasound on bacterial membrane potential.

hyperpolarization arose from changes in cell membrane permeability and the diffusion of potassium ions from the inside to the outside of the cell following ultrasound application [35]. In addition to ions, macromolecular electrolytes like proteins could have leaked into the supernatant of the bacterial suspension as a result of the breakdown and disruption of the bacterial cell wall membrane, thereby increasing conductivity [36]. These results suggested that ultrasound increased the membrane potential of bacteria, leading to hyperpolarization, which affected the bacteria's normal physiological metabolic activities subsequently. Notably, the membrane potential of *S. baltica* significantly increased at 7.5 min of ultrasonic treatment, while that of *A. veronii* significantly increased at 12.5 min, suggesting that *A. veronii* exhibits greater ultrasound resistance compared to *S. baltica*.

3.6. Effect of ultrasound on cell membrane fluidity

Cell membrane fluidity is an important factor in maintaining cell functions, including cell division, diffusion, energy production and maintenance of ion pumping [37]. Therefore, alterations in cell membrane fluidity can serve as an indicator of the impact of ultrasound on cell physiological activities to some extent. ANS, as a fluorescent probe, can attach to the hydrophobic regions on the bacterial cell membrane. Generally speaking, the higher the fluorescence intensity, the worse the fluidity of cell membrane. As depicted in Fig. 5, the fluidity of the cell membrane in *S. baltica* following ultrasonic treatment was notably lower compared to the control group, reaching its minimum at 15 min with prolonged ultrasound exposure. The fluidity of the cell membrane in *A. veronii* decreased not obvious after 5 min of ultrasonic treatment, and it was significantly decreased after 10 min. Cell membrane fluidity was affected by the content of unsaturated fatty acids in the phospholipid bilayer of the cell membrane; the higher the content of unsaturated fatty acids, the greater the fluidity of the cell membrane. At the same time, ultrasonic treatment produced a large number of reactive oxygen species in the hydrophobic zone, leading to a decline in cell membrane fluidity, thus affecting the fluidity of the cell membrane [38]. The study by He et al. [39] indicated a decrease in membrane fluidity of *Escherichia coli* in response to ultrasonic.

3.7. Effect of ultrasound on the ultrastructure of bacterial cell

To enable a more precise observation of the effects of ultrasound on bacterial morphology and structure, transmission electron microscopy (TEM) was utilized to assess the microstructural changes in bacteria following ultrasonic treatment. As shown in Fig. 6, bacteria in the control group exhibited normal morphology, featuring smooth, intact cell membranes and uniformly distributed cytoplasm. In contrast, the ultrasonic treatment caused significant morphological changes. After 5-min exposure, *S. baltica* displayed cell deformation, ruptured cell membranes, and large electron-transparent areas within the cells, with some cells lysing into fragments. A prolonged 15 min treatment led to even greater cell damage, with nearly all cells lysing into debris. The destructive effect of ultrasound on cell membrane was closely related to the treatment time. It could be clearly seen that a short time of ultrasound caused cell deformation, and the cell membrane was partially destroyed, while a longer time of ultrasound completely changed the cell morphology, and most of the cells broke into fragments and were difficult to recognize. However, a comparison between the two bacterial strains indicated that ultrasonic treatment had a more significant destructive effect on the microstructure of *S. baltica*. TEM images revealed that *A. veronii* had a thick cell wall and an outer capsule. This protective capsule provided *A. veronii* with greater resistance to ultrasonic treatment, enabling some bacteria to retain their basic cellular morphology even after extended exposure. Gao et al. [19] also confirmed that the bacterial capsular layer significantly hinders the effectiveness of ultrasound. This observation further elucidated the reason for the relatively low inactivation efficacy of ultrasonic treatment on *A. veronii*.

3.8. The opening of bacterial mechanosensitive ion channels under ultrasonic stress

Mechanosensitive channels, which are integral membrane proteins found in bacteria, archaea and eukaryotes, typically remain closed but open in response to mechanical membrane stretching [40]. When cells are affected by external pressure, the mechanical stress on the cell membrane changes. At that time, the mechanosensitive channels open and release osmotic substances to relieve the increased swelling pressure and prevent cells from bursting [41]. The qPCR results of mechanosensitive ion channel genes of the two bacteria after ultrasonic treatment were shown in Table 4 and Table 5. After 5 min of ultrasonication, the relative gene expression levels of *mscL* and *mscS* in *S. baltica* increased by 0.375 and 1.024, respectively. In contrast, the levels of *mscK*, *mscM*, and *mscL* in *A. veronii* increased by 0.062, 0.196, and 0.032, respectively. This suggested that under ultrasound pressure, *S. baltica* initiated a stress mechanism in response to changes in osmotic pressure. The mechanical stress generated by ultrasound on the cell membrane induces bacteria into a stress state, leading to the regulation of internal gene expression (Fig. 7). This regulation enhanced the expression of mechano-sensitive ion channel genes and activated mechano-sensitive ion channels [18].

However, the genes of *A. veronii* continued to be upregulated with the increase of treatment time, indicating that *A. veronii* was more tolerant to ultrasound, might have been due to the protective effect of its cell capsule on the bacteria mentioned above [42]. This protective mechanism somewhat impeded the conversion of ultrasound external

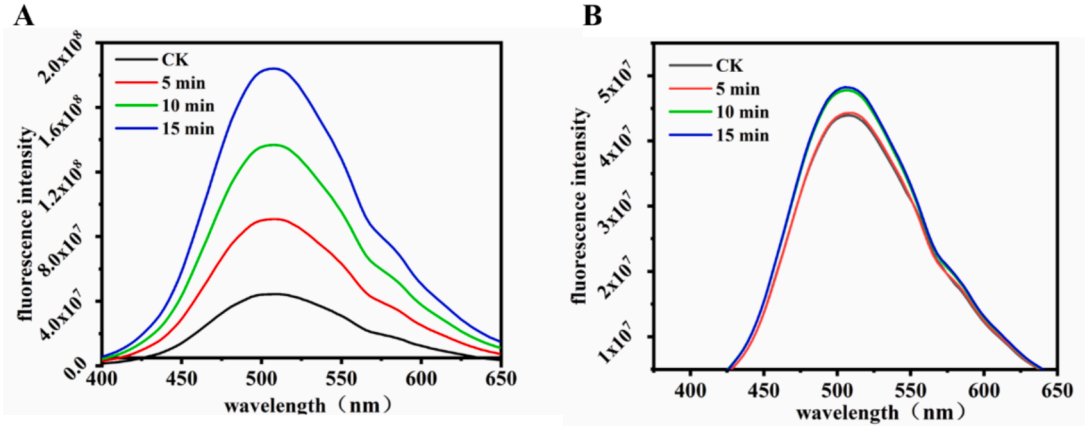

Fig. 5. Effect of ultrasound on cell membrane fluidity of *S. baltica* (A) and *A. veronii* (B).

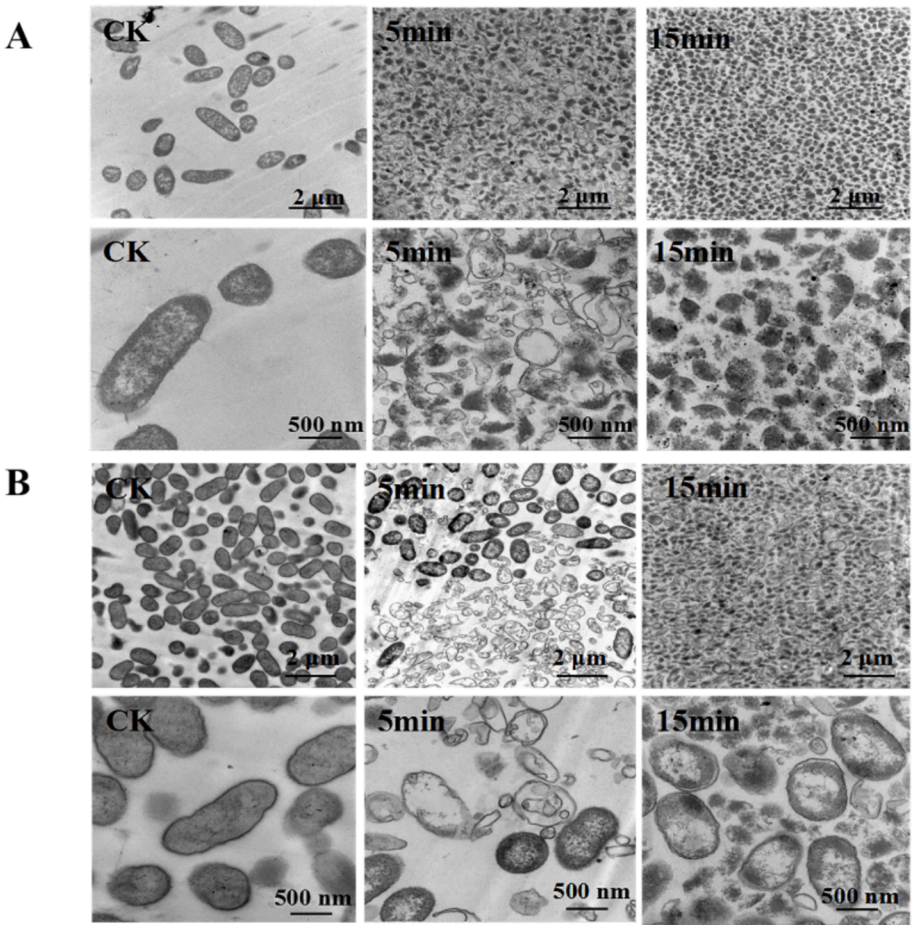

Fig. 6. TEM images of *S. baltica*(A) and *A. veronii*(B) cells.

Table 4
Qpcr verification of target gene expression in *S. baltica.*

gene name	Changes of target gene expression in *S. baltica*			
	US 5 min		US 15 min	
mscS	0.375	up	−0.234	down
mscL	1.024	up	−0.704	down
sucC	1.387	up	−5.361	down
sdhA	9.538	up	−12.212	down

Table 5
qPCR verification of target gene expression in *A. veronii.*

gene name	Changes of target gene expression in *A. veronii*			
	US 5 min		US 15 min	
mscK	0.062	up	0.142	up
mscM	0.196	up	0.576	up
. *mscL*	0.032	up	0.061	up
sucC	0.589	up	0.816	up
sdhA	0.014	up	0.065	up

forces into mechanical stress on the cell membrane. Consequently, mechano-sensitive channel gene expression in *A. veronii* was not significantly increased by short sonication. However, following a longer sonication duration (15 min), the expression of mechano-sensitive channel in *S. baltica* exhibited a declining trend. We speculated that this decline resulted from prolonged sonication leading to cellular stress failure, with most bacteria being killed and intracellular genes and proteins sustaining significant damage. The MS gene in *A. veronii*

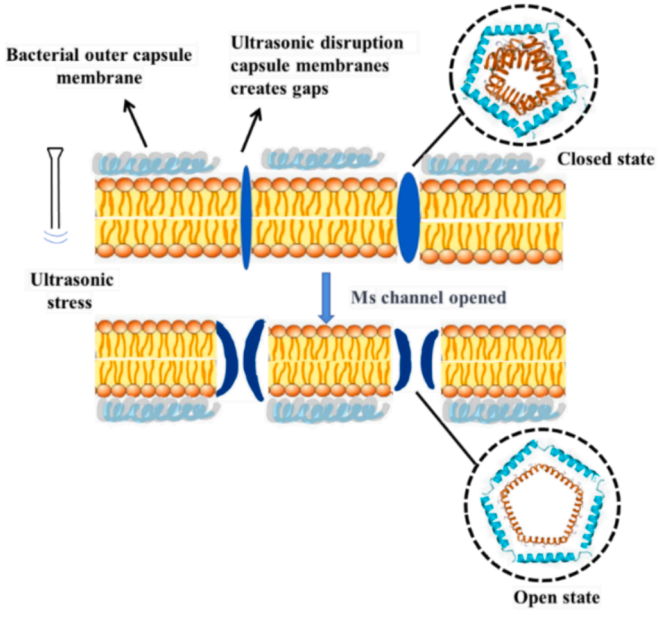

Fig. 7. Schematic diagram of *A.veronii* mechanosensitive channel opening under ultrasonic stimulation.

exhibited a sustained increase, this upregulation could be attributed to the prolonged sonication-induced disruption of outer capsule layer. Concurrently, bacteria perceived mechanical stress at the cell

membrane, which was transformed by the ultrasonic force in the ruptured capsule area, and responded by activating mechanosensitive ion channels to modulate stress. In conclusion, the outer capsule of *A. veronii* effectively served as a protective barrier for the bacteria, relieving the transformation of ultrasonic external forces into cell membrane stress and consequently delaying the process of mechanosensitive ion channel stress mechanism(Fig. 7). Additionally, the expression of *sucC* and *sdhA*, two key enzymes in the tricarboxylic acid cycle of energy metabolism, was up-regulated. This up-regulation was presumably due to the bacteria requiring significant ATP support during their stress response.

4. Conclusion

This study demonstrated that ultrasound treatment had a notable inactivation effect on spoilage bacteria, with a significantly more pronounced bactericidal effect on *S. baltica* than *A. veronii.* After ultrasonic treatment, the integrity of the cell membrane was severely damaged and the cell membrane potential was hyperpolarized, resulting in abnormal cell survival; the fluidity of cell membrane was reduced, the activity of SQR on cell membrane was destroyed. Simultaneously, TEM observations revealed that possessed a thicker cell wall and an outer capsule, which conferred a protective effect. The qPCR data demonstrated that ultrasound induced mechanosensitive ion channel protein up-regulation and channel opening through the cell membrane stress conversion effect. We found that both *S. baltica* and *A. veronii* mitigated ultrasonic stress via mechanosensitive channel proteins; however, they could not prevent membrane destruction after prolonged ultrasonic treatment. The outer capsule of *A. veronii* provided effective protection, delaying the activation of the bacterial mechanosensitive ion channel. The findings on bacterial stress response mechanisms to ultrasound allowed for the optimization of ultrasonic parameters, which could more effectively inactivate *S. baltica* and *A. veronii* in aquatic products.

CRediT authorship contribution statement

Zechuan Dai: Writing – review & editing, Writing – original draft, Visualization, Resources, Methodology, Data curation. **Lingyun Meng:** Writing – original draft, Visualization, Validation, Software. **Sai Wang:** Resources, Project administration, Methodology, Investigation. **Jiao Li:** Writing – review & editing, Supervision, Resources, Project administration, Methodology, Investigation, Funding acquisition, Formal analysis, Data curation. **Xiangzhao Mao:** Writing – review & editing, Resources, Methodology, Investigation, Funding acquisition, Formal analysis, Data curation.

Declaration of competing interest

The authors declare that they have no known competing financial interests or personal relationships that could have appeared to influence the work reported in this paper.

Acknowledgements

This work was supported by the National Key R&D Program of China (2023YFD2401502); National Natural Science Foundation of China (32102130); Natural Science Foundation of Shandong Province (ZR2021QC146) and China Agriculture Research System of Ministry of Finance (MOF) the earmarked fund for CARS-48.

References

[1] G.C. Mair, M. Halwart, Y. Derun, B.A. Costa-Pierce, A decadal outlook for global aquaculture, J World Aquac Soc. 54 (2023) 196–205.
[2] Y. Chu, J. Wang, J. Xie, Foodomics in aquatic products quality assessment during storage: An advanced and reliable approach, Food Biosci. (2024) 103734.
[3] J. Han, Y. Sun, T. Zhang, C. Wang, L. Xiong, Y. Ma, N. Jiang, The preservable effects of ultrasound-assisted alginate oligosaccharide soaking on cooked crayfish subjected to Freeze-thaw cycles, Ultrason. Sonochem. 92 (2023) 106259.
[4] X. Liu, D. Li, K. Li, Y. Luo, Monitoring bacterial communities in ε-Polylysine-treated bighead carp (*Aristichthys nobilis*) fillets using culture-dependent and culture-independent techniques, Food Microbiol. 76 (2018) 257–266.
[5] X. Sun, H. Hong, S. Jia, Y. Liu, Y. Luo, Effects of phytic acid and lysozyme on microbial composition and quality of grass carp (*Ctenopharyngodon idellus*) fillets stored at 4°C, Food Microbiol. 86 (2020) 103313.
[6] X. Yang, W. Lan, X. Sun, Effect of chlorogenic acid grafted chitosan on microbiological compositions of sea bass (*Lateolabrax japonicus*) fillets: Dominant spoilage bacteria, inhibition activity and membrane damage mechanisms, Int. J. Food Microbiol. 411 (2024) 110540.
[7] L. Meng, Z. Dai, J. Li, et al., Screening and identification of dominant spoilage organisms and analysis of bacterial community structure and diversity in refrigerated crayfish, Meat Res. 36 (2022) 16–22.
[8] J. Ma, L. Meng, S. Wang, J. Li, X. Mao, Inactivation of Vibrio parahaemolyticus and retardation of quality loss in oyster (*Crassostrea gigas*) by ultrasound processing during storage, Food Res. Int. 168 (2023) 112722.
[9] A.D. Alarcon-Rojo, L.M. Carrillo-Lopez, R. Reyes-Villagrana, M. Huerta-Jimenez, I. A. Garcia-Galicia, Ultrasound and meat quality: A review, Ultrason. Sonochem. 55 (2019) 369–382.
[10] C.O. Perera, M.A.J. Alzahrani, Ultrasound as a pre-treatment for extraction of bioactive compounds and food safety: A review, LWT - Food Sci. Technol. 142 (2021) 111114.
[11] C. Liu, Q. Xu, J. Ma, S. Wang, J. Li, X. Mao, Ultrasonic cavitation induced *Vibrio parahaemolyticus* entering an apoptosis-like death process through SOS response, Ultrason. Sonochem. 103 (2024) 106771.
[12] J. Li, J. Ahn, D. Liu, S. Chen, X. Ye, T. Ding, Evaluation of ultrasound-induced damage to *Escherichia coli* and *Staphylococcus aureus* by flow cytometry and transmission electron microscopy, Appl. Environ. Microbiol. 82 (2016) 1828–1837.
[13] Q. He, D. Liu, M. Ashokkumar, X. Ye, T.Z. Jin, M. Guo, Antibacterial mechanism of ultrasound against *Escherichia coli*: Alterations in membrane microstructures and properties, Ultrason. Sonochem. 73 (2020) 105509.
[14] N.S.M. Yusof, B. Babgi, Y. Alghamdi, M. Aksu, J. Madhavan, M. Ashokkumar, Physical and chemical effects of acoustic cavitation in selected ultrasonic cleaning applications, Ultrason. Sonochem. 29 (2016) 568–576.
[15] G. Wang, W. Wu, J.J. Zhu, D. Peng, The promise of low-intensity ultrasound: A review on sonosensitizers and sonocatalysts by ultrasonic activation for bacterial killing, Ultrason. Sonochem. 79 (2021) 105781.
[16] S. Drakopoulou, S. Terzakis, M.S. Fountoulakis, D. Mantzavinos, T. Manios, Ultrasound-induced inactivation of gram-negative and gram-positive bacteria in secondary treated municipal wastewater, Ultrason. Sonochem. 16 (2009) 629–634.
[17] B. Krasovitski, V. Frenkel, S. Shoham, E. Kimmel, Intramembrane cavitation as a unifying mechanism for ultrasound-induced bioeffects, Proc. Natl. Acad. Sci. u.s.a. 108 (2011) 3258–3263.
[18] N. Bavi, D.M. Cortes, C.D. Cox, et al., The role of MscL amphipathic N terminus indicates a blueprint for bilayer-mediated gating of mechanosensitive channels, Nat. Commun. 7 (2016) 11984. [19] S. Gao, G.D. Lewis, M. Ashokkumar, Y. Hemar, Inactivation of microorganisms by low-frequency high-power ultrasound: 1. Effect of growth phase and capsule properties of the bacteria, Ultrason. Sonochem. 21 (2014) 446-453.
[19] D.K. Kim, D.H. Kang, Efficacy of light-emitting diodes emitting 395, 405, 415, and 425 nm blue light for bacterial inactivation and the microbicidal mechanism [J], Food Res. Int. 141 (2021) 110105.
[20] J. He, Z. Yang, B. Hu, X. Ji, Y. Wei, L. Lin, Q. Zhang, Correlation of polyunsaturated fatty acids with the cold adaptation of *Rhodotorula glutinis*, Yeast 32 (2015) 683–690.
[21] E.R. Cho, D.H. Kang, Development and investigation of ultrasound-assisted pulsed ohmic heating for inactivation of foodborne pathogens in milk with different fat content, Food Res. Int. 179 (2024) 113978.
[22] M. Cameron, L.D. Mcmaster, T.J. Britz, Electron microscopic analysis of dairy microbes inactivated by ultrasound, Ultrason. Sonochem. 15 (2008) 960–964.
[23] G. Huang, S. Chen, C. Dai, et al., Effects of ultrasound on microbial growth and enzyme activity, Ultrason. Sonochem. 37 (2017) 144–149.
[24] X. Liao, J. Li, Y. Suo, S. Chen, X. Ye, D. Liu, T. Ding, Multiple action sites of ultrasound on *Escherichia coli* and *Staphylococcus aureus*, Food Sci. Hum. 7 (2018) 102–109.
[25] V.D. Badwaik, L.M. Vangala, D.S. Pender, et al., Size-dependent antimicrobial properties of sugar-encapsulated gold nanoparticles synthesized by a green method, Nanoscale Res. Lett. 7 (2012) 1–11.
[26] J.E. Hyun, S.Y. Lee, Antibacterial effect and mechanisms of action of 460–470 nm light-emitting diode against *Listeria monocytogenes* and *Pseudomonas fluorescens* on the surface of packaged sliced cheese, Food Microbiol. 86 (2020) 103314.
[27] W. Jiang, K. Yang, R.W. Vachet, B. Xing, Interaction between oxide nanoparticles and biomolecules of the bacterial cell envelope as examined by infrared spectroscopy, Langmuir 26 (2010) 18071–18077.
[28] N. Fujioka, Y. Morimoto, T. Arai, K. Takeuchi, M. Yoshioka, M. Kikuchi, Differences between infrared spectra of normal and neoplastic human gastric cells, Spectroscopy 18 (2004) 59–66.
[29] R. Moghimi, A. Aliahmadi, H. Rafati, Ultrasonic nanoemulsification of food grade trans-cinnamaldehyde: 1, 8-Cineol and investigation of the mechanism of antibacterial activity, Ultrason. Sonochem. 35 (2017) 415–421.
[30] V. Yankovskaya, R. Horsefield, S. Tornroth, C. Luna-Chavez, H. Miyoshi, C. Léger, S. Iwata, Architecture of succinate dehydrogenase and reactive oxygen species generation, Science 299 (2003) 700–704.

[31] J. Li, L. Ma, X. Liao, D. Liu, X. Lu, S. Chen, et al., Ultrasound-induced Escherichia coli O157.
[32] cell death exhibits physical disruption and biochemical apoptosis, Front. Microbiol. 9 (2018) 2486.
[33] M.J. Jeon, J.W. Ha, Inactivating foodborne pathogens in apple juice by combined treatment with fumaric acid and ultraviolet-A light, and mechanisms of their synergistic bactericidal action, Food Microbiol. 87 (2020) 103387.
[34] C.S. Lunde, S.R. Hartouni, J.W. Janc, M. Mammen, P.P. Humphrey, B.M. Benton, Telavancin disrupts the functional integrity of the bacterial membrane through targeted interaction with the cell wall precursor lipid II, Antitimicrob Agents Ch. 53 (2009) 3375–3383.
[35] C. Bot, C. Prodan, Probing the membrane potential of living cells by dielectric spectroscopy, Eur. Biophys. J. 38 (2009) 1049–1059.
[36] W. Luo, J. Wang, Y. Chen, Y. Wang, R. Li, J. Tang, F. Geng, Quantitative proteomic analysis provides insight into the survival mechanism of Salmonella typhimurium under high-intensity ultrasound treatment, Curr. Res. Food Sci. 5 (2022) 1740–1749.
[37] Y. Wu, J. Bai, K. Zhong, Y. Huang, H. Gao, A dual antibacterial mechanism involved in membrane disruption and DNA binding of 2R, 3R-dihydromyricetin from pine needles of *Cedrus deodara* against *Staphylococcus aureus*, Food Chem. 218 (2017) 463–470.
[38] L.H. Wang, X.A. Zeng, M.S. Wang, C.S. Brennan, D. Gong, Modification of membrane properties and fatty acids biosynthesis-related genes in *Escherichia coli* and *Staphylococcus aureus*: Implications for the antibacterial mechanism of naringenin, Biochim. Biophys. Acta Biomembr. 2018 (1860) 481–490.
[39] L. Siroli, F. Patrignani, F. Gardini, R. Lanciotti, Effects of sub-lethal concentrations of thyme and oregano essential oils, carvacrol, thymol, citral and trans-2-hexenal on membrane fatty acid composition and volatile molecule profile of *Listeria monocytogenes*, *Escherichia coli* and *Salmonella enteritidis*, Food Chem. 182 (2015) 185–192.
[40] C. Kung, B. Martinac, S. Sukharev, Mechanosensitive channels in microbes, Annu. Rev. Microbiol. 64 (2010) 313–329.
[41] C. Catalano, D. Ben-Hail, W. Qiu, et al., Cryo-EM structure of mechanosensitive channel YnaI using SMA2000: Challenges and opportunities, Membranes 11 (2021) 849.
[42] M. Sidarta, L. Baruah, M. Wenzel, Roles of bacterial mechanosensitive channels in infection and antibiotic susceptibility, Pharmaceuticals. 15 (2022) 770.